MOLECULAR AND CELLULAR BIOLOGY, Nov. 1998, p. 6325–6339 Vol. 18, No. 11
0270-7306/98/$04.00+0

RhoA-Binding Kinase α Translocation Is Facilitated by the Collapse of the Vimentin Intermediate Filament Network

WUN-CHEY SIN,[1] XIANG-QUN CHEN,[1] THOMAS LEUNG,[1] AND LOUIS LIM[1,2]*

Glaxo-IMCB Group, Institute of Molecular and Cell Biology, Singapore 117609, Singapore,[1] and Institute of Neurology, London WC1N 1PJ, United Kingdom[2]

Received 22 April 1998/Returned for modification 21 May 1998/Accepted 19 August 1998

The regulation of morphological changes in eukaryotic cells is a complex process involving major components of the cytoskeleton including actin microfilaments, microtubules, and intermediate filaments (IFs). The putative effector of RhoA, RhoA-binding kinase α (ROKα), is a serine/threonine kinase that has been implicated in the reorganization of actin filaments and in myosin contractility. Here, we show that ROKα also directly affects the structural integrity of IFs. Overexpression of active ROKα, like that of RhoA, caused the collapse of filamentous vimentin, a type III IF. A RhoA-binding-deficient, kinase-inactive ROKα inhibited the collapse of vimentin IFs induced by RhoA in HeLa cells. In vitro, ROKα bound and phosphorylated vimentin at its head-rod domain, thereby inhibiting the assembly of vimentin. ROKα colocalized predominantly with the filamentous vimentin network, which remained intact in serum-starved cells. Treatment of cells with vinblastine, a microtubule-disrupting agent, also resulted in filamentous vimentin collapse and concomitant ROKα translocation to the cell periphery. ROKα translocation did not occur when the vimentin network remained intact in vinblastine-treated cells at 4°C or in the presence of the dominant-negative RhoAN19 mutant. Transient translocation of ROKα was also observed in cells subjected to heat shock, which caused the disassembly of the vimentin network. Thus, the translocation of ROKα to the cell periphery upon overexpression of RhoAV14 or growth factor treatment is associated with disassembly of vimentin IFs. These results indicate that Rho effectors known to act on microfilaments may be involved in regulating the assembly of IFs. Vimentin when phosphorylated also exhibits reduced affinity for the inactive ROKα. The translocation of ROKα from IFs to the cell periphery upon action by activated RhoA and ROKα suggests that ROKα may initiate its own cascade of activation.

Cells often undergo dramatic cytoskeletal changes in response to extracellular signalling cues. The Rho subfamily of small GTP binding proteins has emerged as the major player in the regulation of actin cytoskeleton (29, 49). Microinjection of family members RhoA, Rac, and Cdc42 into fibroblasts promotes formation of actin microfilament-containing stress fibers, lamellipodia, and filopodia, respectively (42, 58, 61, 62). They also mediate actin reorganization in various processes such as cytokinesis, motility, and exocytosis and play an essential role in growth control and stress responses (71). Several serine/threonine kinases which bind directly to the activated form of the Rho proteins, including p21 Cdc42/Rac binding p21-activated kinase PAK (53), RhoA-binding kinase α (ROKα) (46), and myotonic dystrophy kinase-related Cdc42-binding kinase (48), appear to act as effectors. For example, p21-activated kinase promotes morphological changes in actin-containing structures consistent with a role downstream of GTPases (52, 64). ROKα, which belongs to a family of ~160-kDa ROKs (36, 46, 54), promotes formation of stress fibers and focal adhesion complexes (2, 37, 47), possibly through enhancing myosin contraction by inactivating myosin phosphatase or phosphorylating myosin light chain (MLC) itself (4, 39, 44). ROKα also appears to stimulate transcription activity (11). Recently, RhoA effectors have also been shown to regulate intermediate filaments (IFs). ROKα/Rho-kinase is reported to phosphorylate glial fibrillary acidic protein (GFAP) (41), and protein kinase N (PKN) (3) affects the state of neurofilaments by phosphorylation (56).

The role of RhoA-induced contractility in promoting assembly of focal adhesions and stress fibers is also being actively pursued (7). Agents that increase contractility include growth factors such as lysophosphatidic acid (LPA) and sphingosine-1-phosphate (SPP) and microtubule (MT)-depolymerizing agents such as vinblastine (17). Treatment of cells with these agents drives the formation of RhoA-induced phenotypes such as an increase in stress fiber bundles and focal adhesion assembly (19, 75). All these phenotypes can be blocked by the *Clostridium botulinum* C3 exoenzyme, which ADP ribosylates RhoA and inactivates it. Contractility inhibitors such as butanedione-2-monoxime also inhibit RhoA-induced phenotypes (14), leading to the suggestion that RhoA-stimulated contractility is essential for formation of stress fibers and focal adhesion assembly.

The reorganization of actin filaments is likely to be influenced by other components of the cytoskeleton; the increase in stress fibers when MTs are depolymerized by vinblastine is an example (5). Depolymerization of MTs causes the collapse of type III IFs into a perinuclear cap (23). IFs are one of the three main components of the cytoskeleton. Vimentin, a type III IF protein, is found abundantly in the perinuclear region of the cells. Although IFs appear to have a significant role in maintaining the integrity of cytoplasm, their regulatory mechanism is not well understood. Three separate domains can be identified in most IF proteins: the head, the central helical coiled-coil/rod, and the nonhelical tail domain. The central helical domain appears to interact with other rod domains via hydrophobic interactions to form oligomers (23). However, the head domain seems to be the regulatory region affecting the poly-

* Corresponding author. Mailing address: Glaxo-IMCB Group, Institute of Molecular and Cell Biology, 30 Medical Dr., Singapore 117609, Singapore. Phone: (65) 874-6167. Fax: (65) 774-0742. E-mail: L.Lim@ion.ucl.ac.uk.

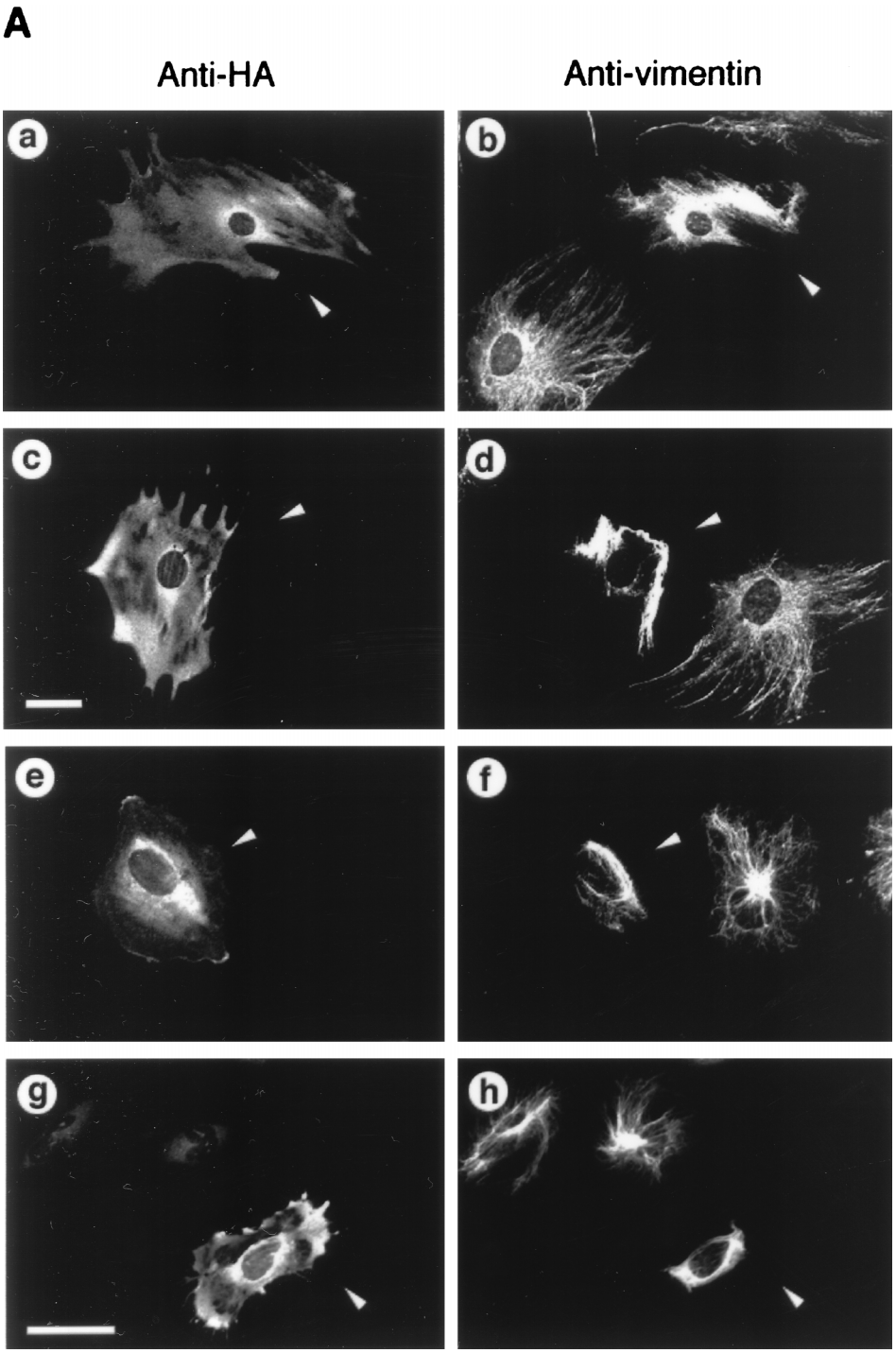

FIG. 1. ROKα is involved in RhoA-induced collapse of IFs. (A) Subconfluent Swiss 3T3 fibroblasts (a to d) were cultured on glass coverslips and microinjected with plasmid encoding HA-tagged full-length wild-type ROKα (a and b) or the kinase domain of ROKα(1–543) (c and d). HeLa cells (e to h) were similarly injected with DNA encoding full-length wild-type HA-tagged ROKα (e and f) or the kinase domain of ROKα(1–543) (g and h). Two hours after incubation, cells were fixed and double stained with anti-HA antibody (a, c, e, and g) and antibodies against vimentin (b, d, f, and h) to detect injected cells (arrowheads). (B) Subconfluent HeLa cells were cultured on glass coverslips and microinjected first with plasmid encoding kinase-dead, RhoA-binding-deficient HA-tagged ROKαK112A/N1027T/K1028T mutant (c to f). Two hours later, some of these cells were also injected with GST-RhoAG12V and incubated for 20 min (e and f). Control cells were injected with GST-RhoAG12V (a and b) and ROKα mutant construct alone (c and d). Cells were fixed and stained with antibodies against vimentin (b, d, and f) and double stained with either rhodamine-conjugated anti-HA to detect cells expressing ROKαK112A/N1027T/K1028T (c) or rhodamine-conjugated anti-GST to detect cells injected with GST-RhoAG12V (a and e). Arrowheads indicate the injected cells located by HA or GST staining and visualized by confocal microscopy. Bars = 15 μm.

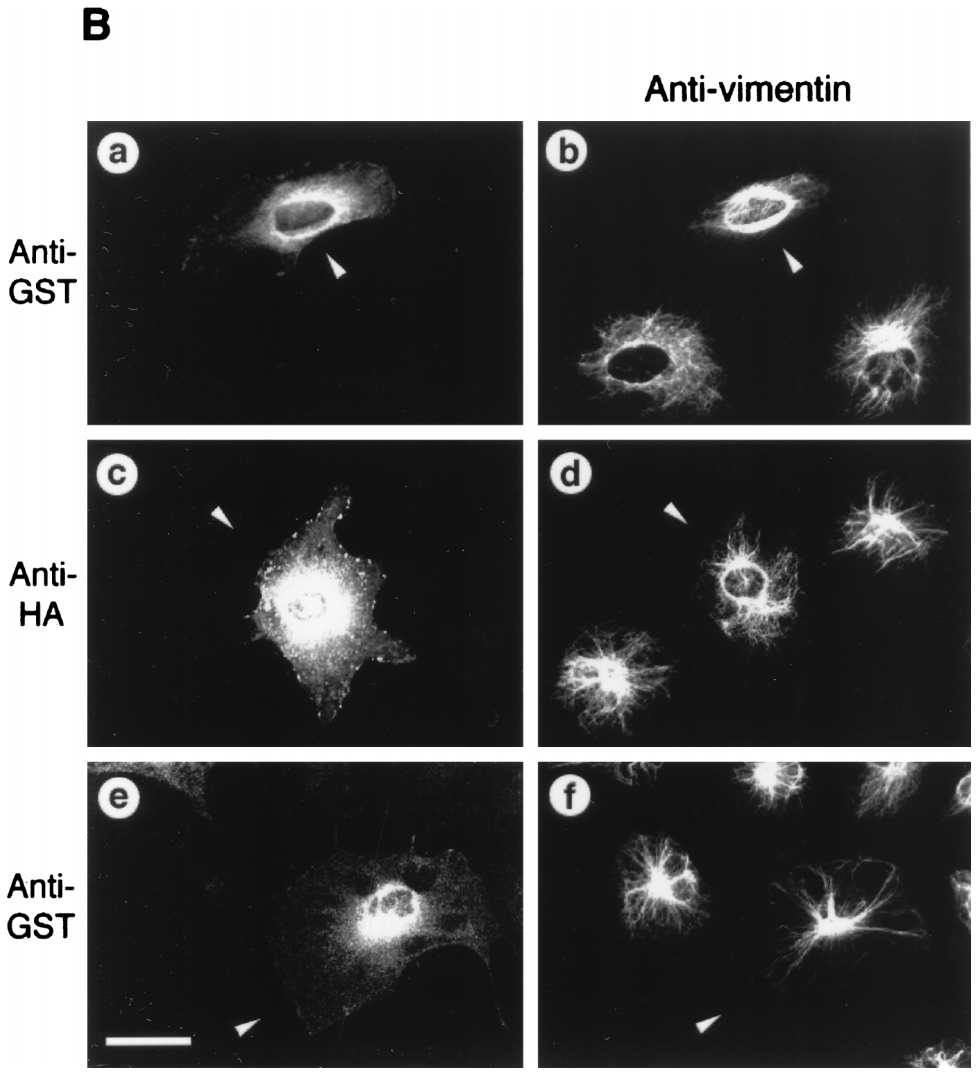

FIG. 1—*Continued.*

merization of IFs (68). Vimentin is an excellent in vitro target of a number of kinases, notably protein kinase A (PKA), protein kinase C (PKC), and cdc2 (34). Reorganization of IFs comprising vimentin during mitosis is thought to be mediated by phosphorylation of its head domain by cdc2 (20). The phosphorylation of vimentin by kinases, which include some RhoA effectors (41, 56), appears to be a major mediator of the dynamics of IFs, and the assembly of IFs is likely to affect the stability of other major cytoskeletal systems.

Here we report that ROKα acts as a common effector of RhoA in promoting reorganization of both microfilaments and IFs. Overexpression of ROKα caused the collapse of vimentin-containing IFs. Regulating the state of vimentin IFs by phosphorylation appears to provide a means of affecting the distribution of ROKα. Endogenous ROKα colocalized preferentially with the vimentin network in serum-starved cells. The collapse of IFs caused by activated ROKα resulted in the release of IF-bound ROKα, which was subsequently translocated from the vimentin network to the peripheral sites. The results suggest a novel mechanism in which the IFs are utilized by a RhoA effector kinase to regulate its own distribution.

MATERIALS AND METHODS

Microinjection and transfection. HeLa cells were transfected by the calcium phosphate method (9). Microinjections and subsequent immunostaining were carried out as described by Leung et al. (47). Briefly, subconfluent cells plated on coverslips for 48 h in minimal essential medium with 10% fetal bovine serum (FBS) were microinjected with plasmid DNA (50 ng/μl) by using an Eppendorf micromanipulator system. Two hours after injection, cells were fixed with 3.7% paraformaldehyde and incubated in phosphate-buffered saline (PBS)–0.5% Triton X-100 for 2 h at 25°C with various primary antibodies: antihemagglutinin (anti-HA) (Santa Cruz) and either anti-vimentin monoclonal antibody (MAb) (vim13.2; Sigma; 1:200) or antivinculin MAb (hVIN-1; Sigma; 1:200), followed by secondary antibodies of rhodamine-conjugated anti-rabbit immunoglobulin G (IgG) (1:50; Boehringer Mannheim) and fluorescein isothiocyanate (FITC)-conjugated anti-mouse IgG (1:100; Boehringer Mannheim) for 1 h at 25°C. In some experiments, when glutathione *S*-transferase (GST) fusion protein (RhoAG14V; 0.2 μg/μl) was injected 2 to 3 h after the first plasmid injection, cells were double stained with rabbit anti-GST and mouse antivimentin 20 min postinjection.

Immunofluorescence microscopy. Swiss 3T3 fibroblasts were cultured in chamber slides in Dulbecco's modified Eagle's medium with 10% FBS. HeLa cells were cultured in minimal essential medium containing 10% FBS. They were serum starved for 24 h and were either left untreated or treated with SPP (Sapphire Bioscience) at 1 μM for 20 min or vinblastine (Sigma) at 50 μg/ml for 40 min. Treated cells were washed once with PBS, fixed with 3.7% paraformaldehyde for 20 min, and permeabilized in 0.5% Triton X-100 for 10 min. Methanol with the addition of 5 mM EDTA was also used as a fixing agent at −20°C

for 10 min. For single staining of vimentin, antivimentin MAb (1:200; Sigma) was used. For double-staining experiments, the fixed cells were incubated simultaneously with mouse anti-ROKα antibody 1A1 (46) and goat antivimentin (1:50; Sigma). The slides were washed with PBS–0.1% Triton X-100 and incubated with appropriate secondary antibodies; FITC-conjugated anti-mouse IgG (1:100; Boehringer Mannheim) was used for single primary antibody staining, and FITC-conjugated anti-goat IgG (1:100; Sigma) and tetramethyl rhodamine isothiocyanate (TRITC)-conjugated anti-mouse IgG (1:50; Boehringer Mannheim) were used for double staining. Actin filaments were visualized with TRITC-conjugated phalloidin (1 μg/ml; Sigma). MTs were visualized by anti-β-tubulin MAb (TUB 2.1; Sigma; 1:200). In certain cases, the microtubular networks of the cells were disrupted by preincubation with 0.5% Triton X-100 in 10 mM Tris (pH 7.8)–0.14 M NaCl–5 mM $MgCl_2$ for 4 min at 37°C, as described by Osborn and Weber (59), before fixation. In competition experiments, the primary antibody was first incubated at room temperature for 1 h with a fivefold excess of purified vimentin protein or GST protein. Heat shock treatment of HeLa cells was carried out at 43°C for 20 min. Conventional fluorescence microscopy was done with a microscope (model Axioplan2; Carl Zeiss, Inc.) with a 40× 1.3 oil immersion objective. Confocal microscopy was performed with a scan head (model MRC600; Bio-Rad Laboratories) connected to a microscope (model Axiophot; Carl Zeiss, Inc.) with epifluorescence optics.

Expression and purification of recombinant proteins. The recombinant proteins for various domains of ROKα were constructed as follows. The mung bean nuclease blunt-ended *Nde*I fragment of a truncated cDNA (46) containing the helical domain of ROKα (amino acids 321 to 971) was digested with *Eco*RI and subcloned into *Xmn*I-*Eco*RI-digested pMal-c2 vector (New England Biolabs) to be expressed as a 100-kDa maltose-binding protein (MBP) fusion protein. Both the kinase and the kinase-dead domain (KD) MBP fusion were obtained by ligating the *Bam*HI-*Xba*I fragment (amino acids 1 to 468) of full-length ROKα or the full-length mutated ROKα construct (47) into pMal-c2 cut with *Bam*HI-*Xba*I to be expressed as an 80-kDa protein. The *Xmn*I-*Sal*I fragment of an N-terminally truncated cDNA (46) containing the pleckstrin homology (PH)–cysteine-rich domain of ROKα (amino acids 1059 to 1379) was ligated to the *Sma*I-*Sal*I digest of pGEX.4T1 (Pharmacia) to be expressed as a 50-kDa protein. GST-vimentin head domain (amino acids 1 to 120) was obtained by first carrying out a PCR on EST 535450 Bluescript clone with primers T7 and 5′ CTTCGG ATCCATGTCTACCAGGTCTGTG; the PCR fragment was double digested with *Bam*HI-*Xho*I and subcloned into pGEX.4T1 vector similarly digested to be expressed as a 40-kDa protein. The MBP and the GST fusion proteins were purified according to the manufacturer's protocol.

For expression of GST-ROKα full-length protein in insect Sf9 cells, a GST tag was added to the original pfast-Bac vector (Clontech) for easy purification. The *Bam*HI-*Eco*RI fragment (amino acids 1 to 1379) of full-length ROKα in pXJ40 was subcloned into the *Bam*HI-*Eco*RI site of pfast-Bac. To clone the GST cassette into pfast-Bac already carrying the insert, a pair of primers (5′ GAAA CAAGATGTATGTCCCCTATACTAGGTTATTGG and 5′ GAATTCCGGG GATCCACGCGGAACCAG) flanking the 5′ and 3′ ends of the DNA sequence encoding the GST protein was used for the PCR. The 680-bp fragment obtained was double digested with *Bgl*II and *Bam*HI so that it was cloned in frame to the ROKα cDNA at the 5′ *Bam*HI site. Purification of the GST-ROKα was carried out as follows. Insect cells were infected at a multiplicity of infection of 10 and harvested after 48 h. The GST fusion protein was purified with glutathione-Sepharose (Pharmacia) according to the manufacturer's protocol.

Purification of native proteins. The purification of native ROKα from rat brains was carried out as described elsewhere (46). Crude vimentin was obtained from Swiss 3T3 cells and further purified by one cycle of assembly-disassembly, based on the protocol reported by Zackroff and Goldman (74).

In vitro kinase assay. One microgram of vimentin was incubated with 200 ng of kinase for 1 h at 30°C in a reaction mixture containing 25 mM Tris (pH 7.0), 0.5 mM $MgCl_2$, 10 μM ATP, and 10 μCi of [γ-^{33}P]ATP (Amersham). The reaction was stopped by addition of an equal volume of 2× sample buffer and then separated on a sodium dodecyl sulfate–10% polyacrylamide gel electrophoresis (SDS–10% PAGE) gel. The phosphorylated proteins were visualized by autoradiography with Kodak MS film. In some instances, RhoA was preexchanged with either GTPγS [guanosine 5′-*O*-(3-thiotriphosphate)] or GDP, as described by Leung et al. (46), before being added to the kinase mixture. Quantification of the phosphorylation was carried out with an imaging analyzer (Bio-Imager; Kodak). The phosphorylated vimentin in the kinase reaction was cleaved with 2-nitro-5-thiocyanobenzoic acid (NTCB) at its sole cysteine residue, as described by Suga et al. (67), to a 37-kDa head-rod domain and an 18-kDa tail domain. The phosphorylated fragments were then separated by SDS-PAGE and visualized by silver staining and autoradiography.

In vitro polymerization of IFs. The polymerization of IFs was carried out as described by Inagaki et al. (33). Briefly, 5 μg of purified vimentin was first phosphorylated as described above with 200 ng of kinase but in the presence of unlabelled 0.1 mM ATP. To initiate the polymerization, 150 mM NaCl was added and the mixture was incubated at 25°C for 1 h. The filaments were pelleted at 20,000 × *g* for 30 min. The samples were separated by SDS-PAGE and visualized by Coomassie blue staining.

In vitro binding assay. Exogenous vimentin (100 μg/ml) was incubated with 1 μg of various recombinant proteins already coupled to Sepharose beads in the presence of 100 μg of bovine serum albumin (BSA) per ml in buffer V (1% Nonidet P-40, 0.5% deoxycholate, 50 mM NaCl, 5 mM EDTA, 50 mM Tris [pH 7.4], 1 mM dithiothreitol, 1 mM phenylmethylsulfonyl fluoride, 10 μg each of leupeptin and aprotinin per ml). After incubation for 2 h at 4°C, the beads were washed five times with buffer V and the bound proteins were eluted in 2× SDS-Laemmli sample buffer. The proteins were separated on an SDS-PAGE gel and Western transferred to a nitrocellulose filter. The filter was probed with mouse antivimentin antibody, followed by horseradish peroxidase-conjugated anti-mouse antibody (Dako) according to standard procedures, and the bands were visualized with ECL chemiluminescence (Amersham).

Overlay binding assay. The assay was mainly based on the method described by Foisner et al. (21). Briefly, purified vimentin from Swiss 3T3 cells was partially cleaved with chymotrypsin in 5 mM sodium borate buffer (pH 8.5) at a protease/vimentin mass ratio of 1:400 at room temperature for 5 min. Alternatively, recombinant GST-vimentin head domain was phosphorylated by PKA in the presence of 0.1 mM ATP as described above. The samples were then subjected to SDS-PAGE and Western blotted to nitrocellulose filters. The filters were first blocked in buffer containing 0.05% Triton X-100 and 3% BSA in PBS for at least 1 h and then overlaid with 1 μg of either MBP alone or MBP fusion of the ROKα KD (MBP-KD) per ml overnight in 0.05% Triton X-100–1% BSA in PBS at 4°C. For detection of bound MBP-ROKα fusion proteins, the filters were probed with anti-MBP antibody (Santa Cruz) and detected by ECL as described above.

RESULTS

ROKα induces the collapse of IFs. Overexpressed ROKα mimicked RhoA in inducing actin reorganization (2, 37, 47). Microinjection of a DNA plasmid encoding the active kinase domain of ROKα into the nuclei of HeLa cells induced an increase in stress fibers within 2 h. The microtubular network is not affected by overexpression of both RhoA and ROKα (47, 60). However, the activated RhoA mutant, RhoAV14, causes the collapse of vimentin IFs into irregular thick bundles in subconfluent fibroblasts (60). We examined whether ROKα could mediate the effects of RhoA on the vimentin IF network. Microinjection of full-length wild-type ROKα induced the collapse of vimentin IFs in Swiss 3T3 fibroblasts (Fig. 1A, a and b). The IF collapse induced by ROKα is similar to that induced by microinjection of PKA into fibroblasts (45). A truncated ROKα consisting of the kinase domain displayed marked increased kinase activity compared to that of the full-length ROKα (47). Microinjection of this constitutive active kinase into fibroblasts resulted in the complete collapse of the IF network to form a vimentin-containing arc near the perinuclear region when the cell shape remained unchanged (Fig. 1A, c and d). Expression of the microinjected DNA plasmids was confirmed with anti-HA antibody which recognized the fusion tag. Microinjection of full-length ROKα and active kinase domain of ROKα, which were previously used to demonstrate ROKα induction of stress fibers and focal adhesions, also caused the collapse of vimentin IFs in HeLa cells (Fig. 1A, e to h). The greater effectiveness of the kinase domain is related to its enhanced kinase activity. Thus, fibroblasts and HeLa cells were identical in their responses to overexpressed ROKα, and HeLa cells were then used to facilitate analysis of RhoA-induced IF collapse. The complete collapse of vimentin IFs induced by the constitutively active ROKα was comparable to that induced by the activated RhoA mutant, RhoAV14 (Fig. 1B, a and b); therefore, the kinase activity of ROKα is sufficient for inducing the collapse of the IF network in vivo. To determine whether ROKα is acting downstream of RhoA in causing the collapse of vimentin IFs, a kinase-dead, RhoA-binding-deficient mutant (ROKαK112A/N1027T/K1028T) (47) which did not cause the collapse of IFs when overexpressed was used (Fig. 1B, c and d). To coexpress this ROKα mutant with RhoAV14, the HA-tagged plasmid encoding the mutant was injected into HeLa cells 2 to 3 h before the injection of GST-RhoAV14 fusion protein. The presence of kinase-dead, RhoA-binding-deficient ROKα abolished the RhoA-induced IF collapse (Fig. 1B, e and f), probably through the ROKα mutant acting as a dominant-negative inhibitor of endogenous

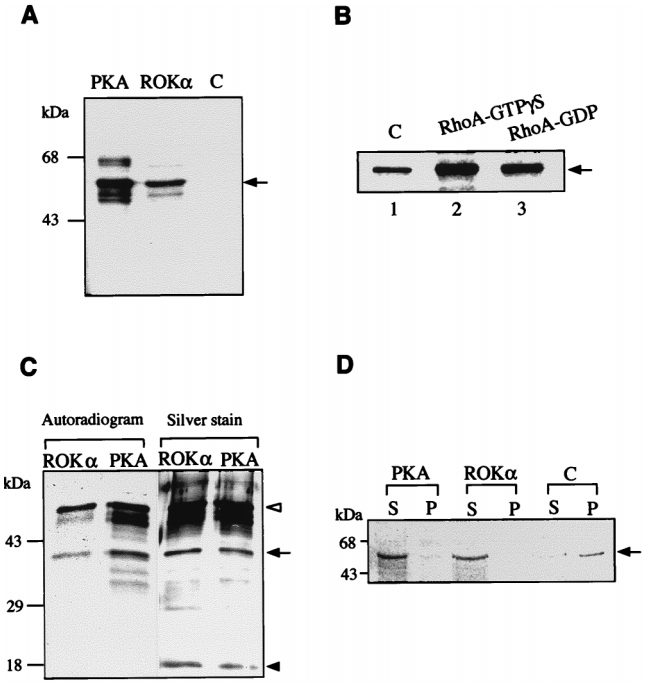

FIG. 2. Phosphorylation of vimentin by ROKα. (A) Phosphorylation was carried out in a standard kinase assay in the presence of 10 μCi of [γ-^{33}P]ATP with 200 ng of ROKα or PKA and 1 μg of purified vimentin (arrow). PKA was used as a positive control. C, negative control without kinase. (B) Kinase assay with 200 ng of GST-ROKα purified from insect cells and 1 μg of vimentin (arrow) in the absence (lane 1) or in the presence of RhoA-GTPγS (lane 2) and RhoA-GDP (lane 3). (C) Vimentin is phosphorylated at its head-rod domain. Vimentin phosphorylated by ROKα and PKA as described for panel A was subjected to NTCB digestion which cleaved vimentin at its only cysteine residue to a 37-kDa head-rod domain (black arrow) and an 18-kDa tail domain (black arrowhead). The phosphorylated fragments were then separated by SDS-PAGE and visualized by silver staining and autoradiography. Undigested vimentin is indicated by a white arrowhead. (D) Effect of phosphorylation on the state of vimentin. Vimentin (5 μg) purified from Swiss 3T3 fibroblasts was first phosphorylated as in the standard kinase assay with either PKA or ROKα in the presence of 0.1 mM ATP. Then it was induced to polymerize in vitro by the addition of 150 mM NaCl, and the mixture was incubated for 1 h at 25°C. Vimentin filaments (arrow) were pelleted at 20,000 × *g* for 30 min. Supernatant (S) and pellet (P) fractions were separated by SDS-PAGE and visualized by Coomassie blue staining. C, control.

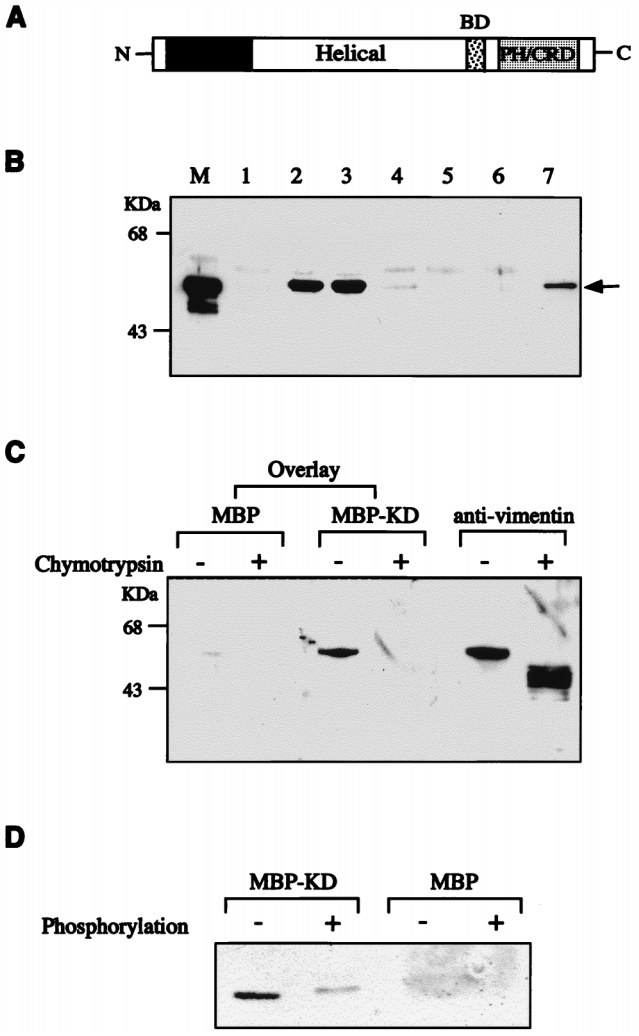

FIG. 3. Association of ROKα and vimentin in vitro. (A) A schematic diagram of ROKα. BD, p21 binding domain; PH/CRD, PH/cysteine-rich domain. (B) Purified vimentin from Swiss 3T3 cells was incubated with MBP or GST fusion proteins containing different domains of ROKα. The lanes include MBP (lane 1), MBP-ROKα kinase domain (lane 2), MBP-ROKα KD (lane 3), MBP-ROKα helical coiled-coil domain (lane 4), GST (lane 5), GST-PH/cysteine-rich domain (lane 6), and GST-full-length ROKα (lane 7). An aliquot of the original mixture was loaded in lane M. The proteins were precipitated with amylose-Sepharose beads (lanes 1 to 4) or glutathione-Sepharose beads (lanes 5 to 7), separated by SDS-PAGE, analyzed by Western blotting, and monitored by ECL to detect the bound vimentin (arrow) with antivimentin antibody. (C) Binding of ROKα to the head domain of vimentin. A filter overlay was carried out on a nitrocellulose filter containing purified vimentin digested in the presence or absence of chymotrypsin. The filter was first overlaid with 1 μg of MBP or MBP-KD (kinase-dead domain of ROKα) (amino acids 1 to 468) per ml and then probed with rabbit anti-MBP and horseradish peroxidase-conjugated anti-rabbit IgG antibodies. The filter was reprobed with antivimentin antibody to confirm the location of the proteins. (D) The ROKα KD has reduced affinity for phosphorylated vimentin. GST-vimentin head domain (1 μg) purified from *E. coli* was phosphorylated in the presence or absence of ATP, subjected to the same overlay treatment with either MBP or MBP-KD as probe as described for panel C, and immunostained with anti-MBP antibody. Film images were digitized with a Microtek scanner, cropped, converted to gray scale with Adobe Photoshop 4.0, and printed with an Epson Stylus Color 800 inkjet printer.

ROKα. This result suggests that ROKα mediates the effect of RhoA in inducing collapse of IFs.

Phosphorylation of vimentin by ROKα. The dynamics of vimentin IFs are regulated by phosphorylation (34), and some of the putative kinases involved are PKA and PKC. Because kinase activity of ROKα is needed for the collapse of IFs, we examined whether vimentin is a substrate of ROKα. Vimentin protofilaments purified from Swiss 3T3 fibroblasts were phosphorylated by native ROKα purified from rat brains (Fig. 2A). Vimentin was phosphorylated less efficiently by ROKα than by PKA, with the phosphorylation stoichiometry of ROKα and PKA being 0.35 and 1.35 mol of phosphate per mol of vimentin, respectively. The molar phosphate incorporated by PKA was consistent with the value obtained by others (35).

We next checked whether the phosphorylation of vimentin by ROKα could be enhanced by the addition of RhoA-GTPγS. The kinase activity of native ROKα could not be further stimulated with RhoA, possibly because of the exposure of ROKα to RhoA-GTPγS used for its purification (46). We therefore expressed recombinant full-length GST-ROKα (180 kDa) in insect cells and then purified it by affinity chromatography with glutathione-Sepharose. This GST-ROKα was active towards vimentin (Fig. 2B, lane 1). The addition of RhoA-GTPγS to the kinase mixture increased the phosphorylation of vimentin by GST-ROKα by 3-fold (Fig. 2B, lane 2) while RhoA-GDP

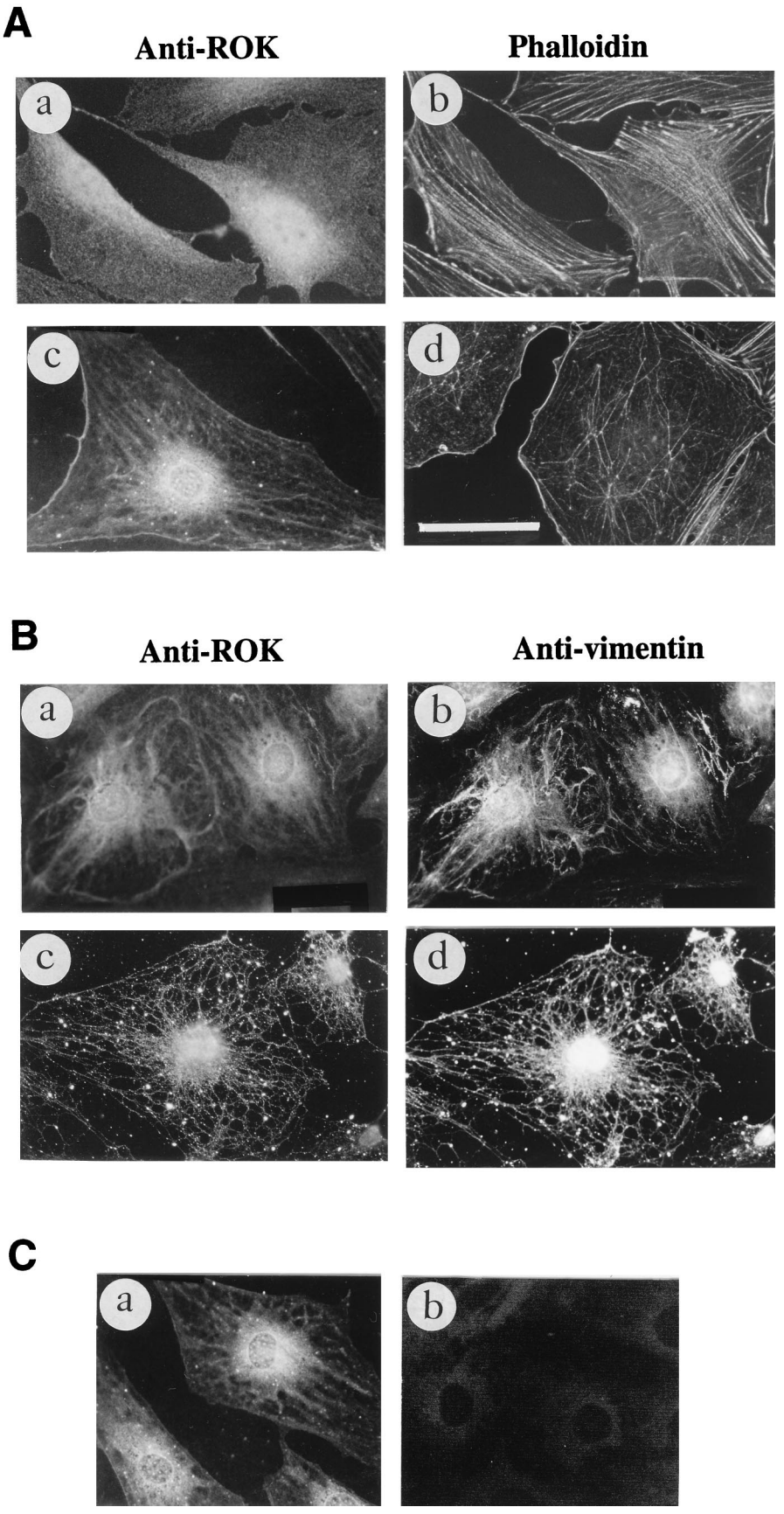
A
Anti-ROK
Phalloidin
a
b
c
d
B
Anti-ROK
Anti-vimentin
a
b
c
d
C
a
b

increased it 1.5-fold (Fig. 2B, lane 3), as determined by densitometry.

To localize the region phosphorylated by ROKα, vimentin was cleaved at its only cysteine residue with NTCB (67). Cleavage of mouse vimentin at this internal cysteine site (8) results in a fragment of 327 amino acids spanning the head-rod region and a fragment of 138 amino acids including the tail domain. PKA was used as a control because it phosphorylates only at the head domain of vimentin (25). Figure 2C shows the phosphorylation pattern of NTCB-digested vimentin. The two upper ROKα-phosphorylated bands correspond to the undigested vimentin and the head-rod domain with an apparent molecular mass of 37 kDa, respectively; both are also present in the PKA-phosphorylated preparation, which in addition contains other phosphorylated products. The lower band with an apparent molecular mass of approximately 18 kDa corresponds to the tail region, which was not phosphorylated by either PKA or ROKα. Thus, ROKα, like PKA, phosphorylated vimentin at its N-terminal head-rod domain.

Phosphorylation of IFs usually resulted in their disassembly in vitro (12, 13, 35). To determine whether phosphorylation of vimentin affects its polymerization ability in a similar fashion, vimentin was first phosphorylated by either PKA or ROKα and polymerization was then initiated in vitro by addition of 150 mM NaCl (33). In preparations not treated with kinase, a substantial amount of vimentin was pelleted down at 20,000 × *g* in 30 min, indicating that vimentin protofilaments had polymerized to form filaments. There was a marked inhibition of the polymerization of vimentin phosphorylated by PKA (which acted as a control) and by ROKα, with most of the vimentin remaining in the supernatant fraction (Fig. 2D). Thus, ROKα affects the state of vimentin by phosphorylation in vitro and in vivo, the latter as shown by the microinjection studies.

ROKα associates with vimentin in vitro. Certain kinases, such as PKC, were reported to phosphorylate and to associate with vimentin (66). To determine whether ROKα could associate with vimentin in vitro, various domains of ROKα expressed in *Escherichia coli* were incubated with vimentin (Fig. 3A and B). Both the KD and the kinase domain of ROKα bound to vimentin (Fig. 3B, lanes 2 and 3). Surprisingly, there was no interaction between rod domains of ROKα and vimentin, the coiled-coil helical domain of ROKα binding weakly to vimentin (Fig. 3B, lane 4). Vimentin did not interact with the C-terminal region of ROKα containing the PH and the cysteine/histidine-rich domains (Fig. 3B, lane 6). The p21 binding domain has no affinity for vimentin (data not shown). Vimentin associated with less affinity with full-length ROKα (Fig. 3B, lane 7); this might be due to possible intramolecular interactions between the domains of ROKα (47), preventing full access of vimentin to its binding sites in ROKα in vitro.

To determine the region in vimentin involved in the association with ROKα, a solid-phase binding assay was carried out. Limited digestion of vimentin with chymotrypsin generates a 40-kDa fragment which is more resistant to the digestion than is the amino terminus (i.e., the head domain) (21). The digested proteins were separated by SDS-PAGE, transferred to a nitrocellulose filter, and then overlaid with the KD of ROKα. As shown in Fig. 3C, MBP fusion of the ROKα KD (amino acids 1 to 468) bound to the undigested vimentin but not to the chymotrypsin-digested vimentin lacking the amino terminus. Thus, we conclude that ROKα bound to the head domain of vimentin, as does PKN, another RhoA-binding serine/threonine kinase (56). To determine whether the phosphorylation state of vimentin affects ROKα binding, an overlay on phosphorylated and unphosphorylated GST-vimentin head domain fusion protein was carried out (Fig. 3D). The binding of the kinase-inactive ROKα to vimentin was markedly reduced upon phosphorylation of the IF protein.

ROKα colocalizes with vimentin filaments in Swiss 3T3 fibroblasts. We then checked whether ROKα could associate with vimentin in intact cells. Immunolocalization was carried out on Swiss 3T3 fibroblasts and HeLa cells. The MAb to the kinase domain of ROKα recognized a single protein in both fibroblasts and HeLa cell extracts (data not shown). ROKα was mainly cytoplasmic in HeLa cells under most culture conditions (see Fig. 5A, a). In contrast, ROKα had a cytoplasmic distribution in actively growing fibroblasts (Fig. 4A, a) and was redistributed to a filamentous structure when the cells were serum starved for 24 h (Fig. 4A, c). The decrease of stress fibers caused by serum deprivation is shown in Fig. 4A, b and d. The same filamentous structure was recognized by antivimentin antibodies (Fig. 4B, a and b) when costaining was carried out. Since MTs and IFs can coalign in some instances (28), the microtubular network was first disrupted with Triton X-100-containing buffer before the cells were fixed (59). The anti-ROKα and antivimentin antibodies recognized virtually identical structures (Fig. 4B, c and d), confirming that ROKα colocalized with vimentin IFs in fibroblasts. However, the staining with anti-ROKα was more discrete than that obtained with antivimentin, dotting the filamentous network. The staining of the filamentous network by anti-ROKα antibody was not due to cross-reactivity of the antibody, since the staining could not be removed with a fivefold excess of vimentin as the competing antigen (Fig. 4C, a), which considerably reduced staining with antivimentin (Fig. 4C, b). Anti-ROKα antibody did not cross-react with vimentin by Western immunoblotting, even at 1-μg levels (data not shown). A separate MAb to ROKα (2G1) also gave the same filamentous pattern in fibroblasts (data not shown).

The collapse of IFs is accompanied by ROKα translocation to the cell periphery. To determine the distribution of ROKα under conditions in which IFs were collapsed, we made use of the MT-depolymerizing agent, vinblastine. The most immediate effect of MT disruption seems to be enhanced contractility, phosphorylation of MLC, and RhoA-mediated increases in stress fibers and focal adhesions (19, 40). All MT-disrupting agents are also known to cause the collapse of type III IFs at the perinuclear cap (23). In HeLa cells, vimentin IFs are the only IFs that collapse in the presence of MT-disrupting agents, while keratin IFs are not affected (22). When HeLa cells were treated with vinblastine, ROKα translocated to the submembranous zone of the cell periphery (Fig. 5A, a and e). There was an accompanying increase in actin stress fibers (Fig. 5A, b and f) and vinculin staining (data not shown) in vinblastine-treated cells, as has been previously shown by others (19, 75). The IFs collapsed (Fig. 5A, c and g) and the MTs depolymerized to form paracrystals (Fig. 5A, d and h) after treatment of the cells with the drug. An identical result was obtained with

FIG. 4. Localization of ROKα to vimentin IFs. (A) Redistribution of ROKα after serum starvation. Swiss 3T3 fibroblasts grown in 10% serum-containing medium for 2 days (a and b) or serum starved for 24 h (c and d) were fixed with methanol and stained with anti-ROKα followed by FITC-conjugated anti-mouse antibody (a and c) or fixed with paraformaldehyde and stained with TRITC-conjugated phalloidin (b and d) to detect actin stress fibers. (B) Confluent Swiss 3T3 fibroblasts grown in serum-free medium for 24 h were double stained with mouse anti-ROKα (a) and goat antivimentin (b). Fibroblasts after extraction with 0.5% Triton X-100 were double stained with mouse anti-ROKα (c) or goat antivimentin (d). (C) Anti-ROKα does not cross-react with vimentin. A competition experiment was performed by incubating the respective primary antibodies with a fivefold excess of purified vimentin and then staining cells with anti-ROKα (a) and antivimentin (b). Bar = 15 μm.

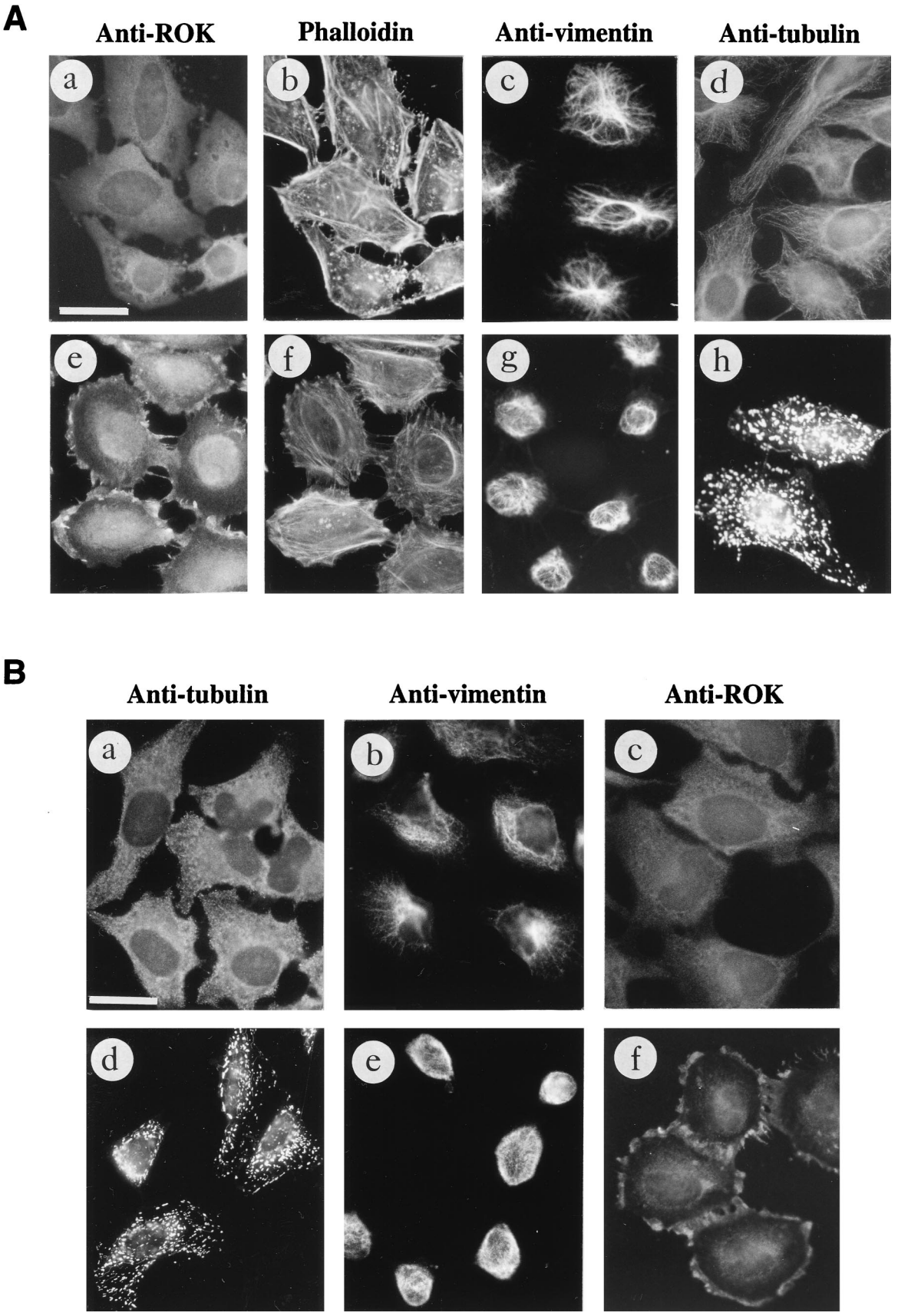
A
Anti-ROK
Phalloidin
Anti-vimentin
Anti-tubulin
a
b
c
d
e
f
g
h
B
Anti-tubulin
Anti-vimentin
Anti-ROK
a
b
c
d
e
f

FIG. 5.

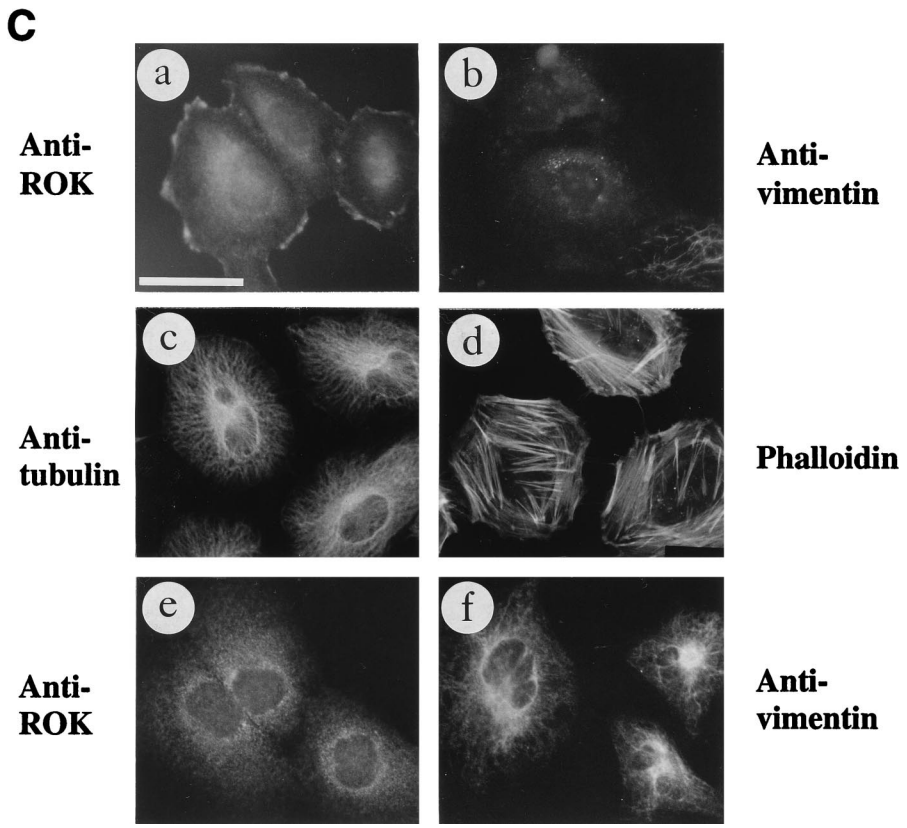

FIG. 5. Collapse of IFs is accompanied by ROKα translocation. (A) Vinblastine induces the collapse of IFs and the translocation of ROKα. HeLa cells were serum starved in 1% FBS overnight and left untreated (a, b, c, and d) or treated with 50 μg of vinblastine per ml for 40 min at 37°C (e, f, g, and h). The cells were stained with anti-ROKα (a and e), TRITC-conjugated phalloidin (b and f), antivimentin (c and g), and antitubulin (d and h) followed by FITC-conjugated anti-mouse IgG and visualized by immunofluorescence. (B) HeLa cells were incubated at 4°C for 1 h (cold treatment), and the cells were treated with 50 μg of vinblastine per ml for a further 20 min at 4°C (a, b, and c) before fixation. Another group of cells similarly treated was allowed to warm up to 37°C in the presence of 50 μg of vinblastine per ml for an additional 40 min (d, e, and f). The cells were stained with anti-β-tubulin (a and d), antivimentin (b and e), and anti-ROKα (c and f), followed by FITC-conjugated anti-mouse IgG. (C) Heat shock causes ROKα to translocate to the cell periphery. HeLa cells were heat shocked for 20 min at 43°C, fixed, and stained with anti-ROKα (a), antivimentin (b), anti-β-tubulin (c), and TRITC-conjugated phalloidin (d). The cells were allowed to recover for 2 h after heat shock and were stained with anti-ROKα (e) and antivimentin (f). Bar = 15 μm.

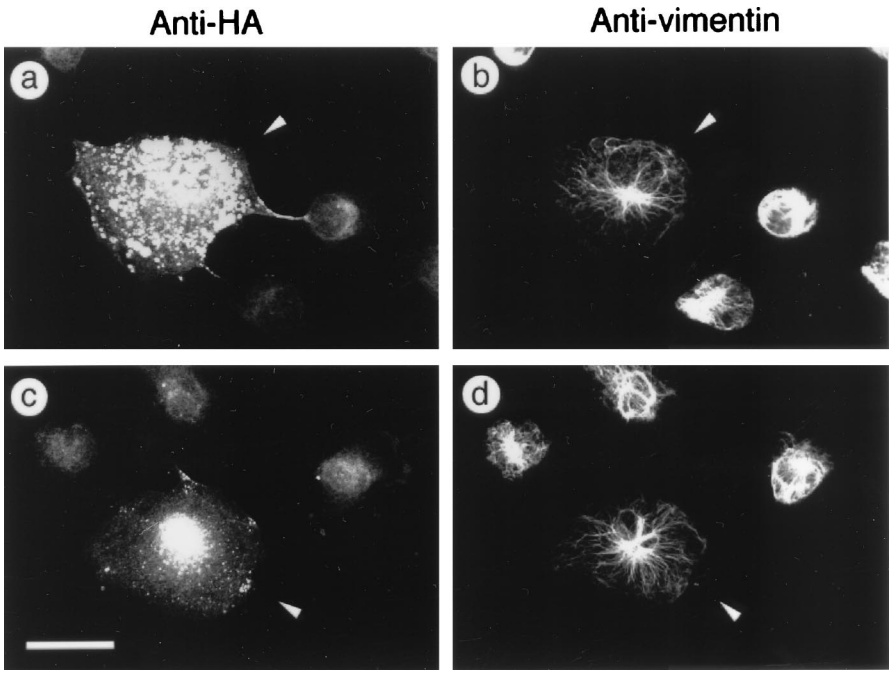

FIG. 6. Kinase activity is required for vinblastine-induced collapse of IFs. HeLa cells were microinjected with plasmid encoding HA-tagged kinase-dead, RhoA-binding-deficient ROKαK112A/N1027T/K1028T (a and b) or HA-tagged RhoAN19 (c and d) for comparison. Two hours after injection, cells were treated with vinblastine for 30 min, fixed with methanol, and costained with rabbit anti-HA antibody (a and c) and mouse antivimentin (b and d) to detect the injected cells (arrowheads). This was followed with rhodamine-conjugated anti-rabbit IgG and FITC-conjugated anti-mouse IgG, and cells were visualized by immunofluorescence. Bar = 15 μm.

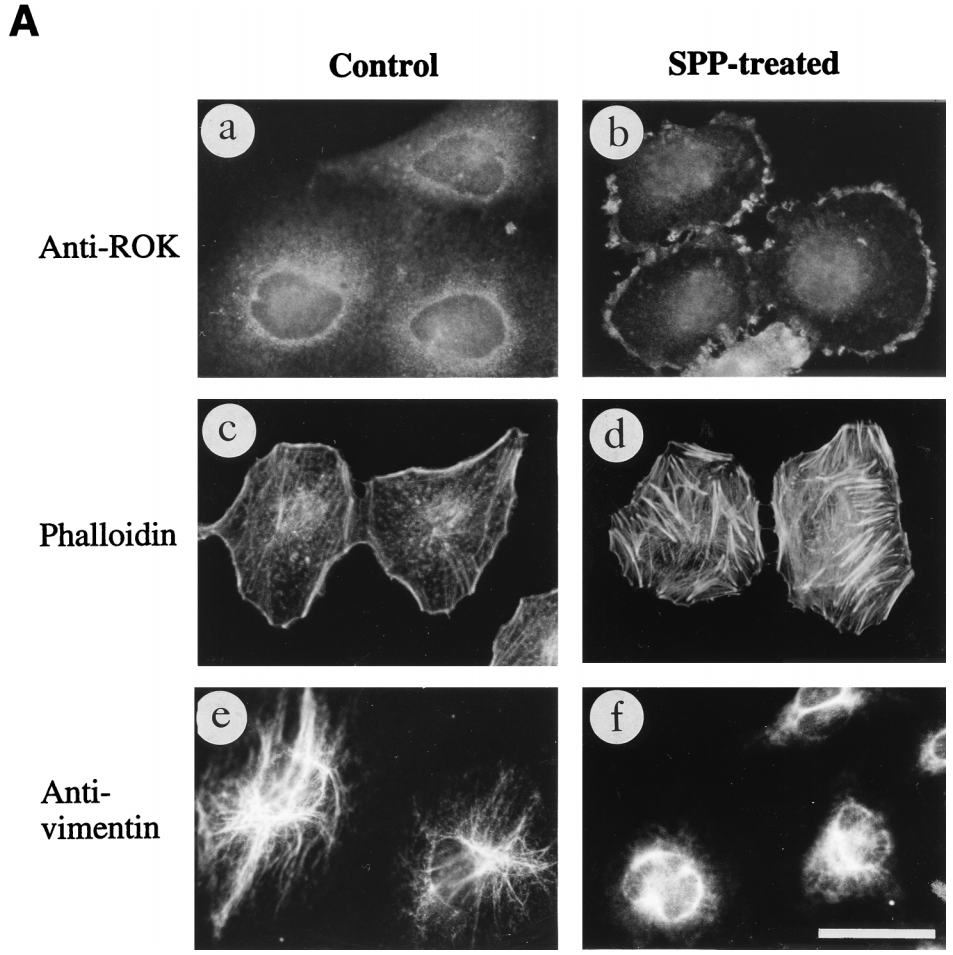

FIG. 7. Activation of RhoA causes a redistribution of ROKα. (A) SPP causes the translocation of ROKα and affects IF stability. HeLa cells were stimulated with SPP at 1 μM for 20 min at 37°C. Cells were fixed with paraformaldehyde and stained with anti-ROKα (a and b) and TRITC-conjugated phalloidin (c and d). Untreated control or SPP-treated cells were stained with antivimentin after methanol fixation (e and f). (B) Translocation of ROKα is inhibited by the dominant-negative RhoAN19 mutant. HeLa cells were transfected with plasmid encoding HA-tagged RhoAN19 and incubated for 24 h. The cells were stimulated with 1 μM SPP for 20 min (a and b) or 50 μg of vinblastine per ml for 40 min (c and d). The cells were fixed and costained with anti-HA (a and c) and anti-ROKα (b and d) to locate the transfected cells. RhoAN19 overexpression (arrowheads) blocked the translocation of ROKα to the cell periphery (arrows). (C) Translocated ROKα overlaps with vinculin staining. HeLa cells were transfected with full-length wild-type HA-tagged ROKα and treated with SPP as described for panel B. Cells were costained with anti-HA (a) and antivinculin (b) to locate the transfected cells. Arrowheads point to transfected cells located by HA staining. Bars = 15 μm.

nocodazole, another MT-depolymerizing drug (data not shown). Thus, depolymerization of MTs was accompanied by the collapse of IFs, an increase in stress fibers, and the redistribution of ROKα to the cell edge. Translocated ROKα was more easily discernible in HeLa cells than in Swiss 3T3 fibroblasts (data not shown); it is not clear whether this is due to the large amount of cytoplasmic ROKα in serum-deprived HeLa cells compared to that in 3T3 cells.

To determine whether the redistribution-translocation of ROKα is due to the collapse of IFs and not to depolymerization of MTs, we exploited the finding that vinblastine at low temperatures does not cause the collapse of IFs although it is still capable of depolymerizing MTs (32). The cells were incubated at 4°C for 1 h before being treated with 50 μg of vinblastine per ml for a further 20 min in the cold. The MT network was not affected by the cold treatment in the absence of drug (data not shown). In the presence of vinblastine at 4°C, MTs were depolymerized (Fig. 5B, a), but the vimentin network remained relatively intact (Fig. 5B, b). ROKα did not translocate to the cell periphery under this condition (Fig. 5B, c), and there was also no increase in stress fibers (data not shown). However, when the cold- and vinblastine-treated cells were further subjected to vinblastine treatment at 37°C for a further 40 min, MTs remained depolymerized and the small crystals previously observed in the cold had fused to form paracrystals of tubulin (Fig. 5B, d). The vimentin network correspondingly collapsed to form a perinuclear arc (Fig. 5B, e), and ROKα translocated to the cell periphery (Fig. 5B, f). Thus, the translocation of ROKα occurred only after the collapse of IFs rather than on depolymerization of MTs. Further evidence of this was provided by heat shock treatment of cells. There are a number of cellular cytoskeletal changes immediately after heat shock, one being the collapse of IFs (72). Treatment of actively growing HeLa cells at 43°C for 20 min caused ROKα to translocate to the cell edge (Fig. 5C, a) and the vimentin network to disassemble into punctate clusters (Fig. 5C, b). The MT and actin networks were not apparently affected (Fig. 5C, c and d). This shows that the disassembly of IFs is sufficient to cause ROKα to translocate to the cell periphery. When the cells were left to recover for 2 h, the IF network started to re-form and ROKα ceased to concentrate at

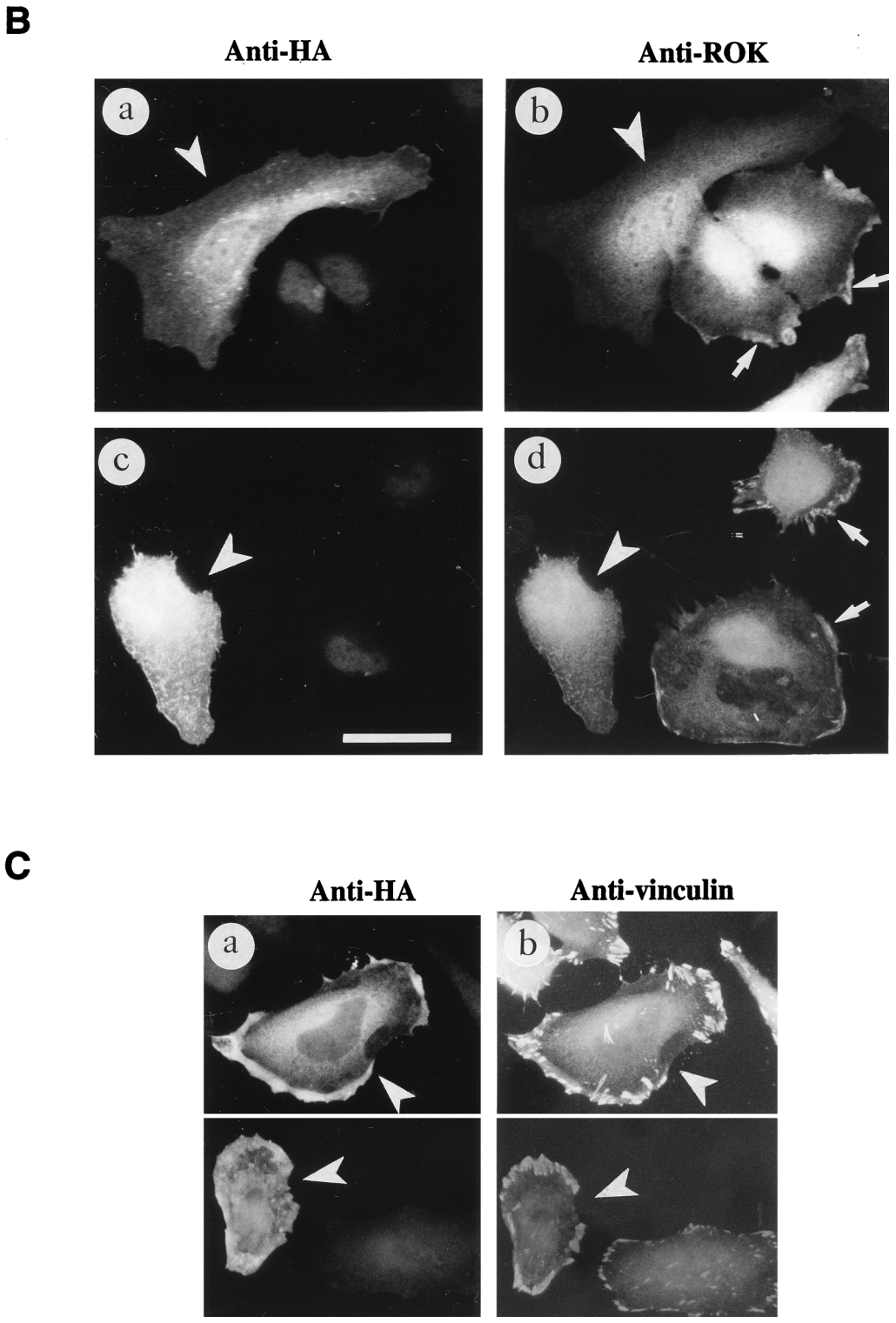

FIG. 7—*Continued.*

the cell periphery, showing that this process was reversible (Fig. 5C, e and f).

ROKα has an active role in the collapse of IFs. We next examined whether ROKα has a direct role in causing the collapse of IFs in vinblastine-treated cells. A plasmid encoding the RhoA-binding-deficient, kinase-dead mutant (ROKαK112A/N1027T/K1028T) was microinjected into HeLa cells, and after 2 h to allow for the expression of the mutant protein, the cells were treated with 50 μg of vinblastine per ml for 40 min. This dominant-negative ROKα inhibited vinblastine-induced col-

lapse of IFs (Fig. 6a and b) but did not inhibit MT depolymerization (data not shown). This indicated that ROKα has an active role in causing the collapse of IFs in vinblastine-treated cells. Similarly, microinjection of the plasmid encoding dominant-negative RhoAN19 blocked the collapse of IFs induced by vinblastine (Fig. 6c and d), consistent with ROKα acting downstream of RhoA in inducing IF collapse.

Redistribution of ROKα in the presence of RhoA-activating agent. MT-depolymerizing agents are known to activate RhoA (19). We then tested growth factors that are known to increase RhoA-GTP level, such as LPA and SPP (50). Treatment of HeLa cells with SPP caused ROKα to translocate to the free edge of subconfluent cells (Fig. 7A, a and b). These cells also showed an increase in stress fibers (Fig. 7A, c and d), as has been previously shown by others. The translocation was still discernible 2 h after SPP treatment, unlike the translocation from the heat shock treatment. Thus, activation of RhoA is necessary for ROKα to remain membrane bound. A similar redistribution of ROKα occurred after the addition of serum or LPA to the cells (data not shown). The vimentin network appeared to contract partially in some SPP-treated cells (Fig. 7A, e and f), perhaps because the stability of IFs in growth factor-treated cells was affected by the increase in the proportion of activated RhoA.

ROKα translocation is RhoA dependent; the overexpression of RhoAN19 dominant-negative mutant abolished both SPP (Fig. 7B, a and b)- and vinblastine (Fig. 7B, c and d)-induced ROKα translocation. RhoAN19 probably sequestered endogenous guanine nucleotide exchange factors and prevented the activation of endogenous RhoA. The dominant-negative RacN17 and Cdc42N17 did not prevent the translocation of ROKα in response to both factors (data not shown). The distribution of the translocated ROKα, when visualized by HA staining of transfected HA-tagged full-length ROKα, appeared to overlap with that of the more discrete focal adhesions as determined by staining of vinculin (Fig. 7C, a and b). Focal adhesions are increased dramatically in the presence of overexpressed ROKα (47). Thus, translocated ROKα accumulated at the cell edge undergoing active cytoskeletal reorganization.

DISCUSSION

The RhoA binding kinases have been implicated in the phosphorylation of the myosin binding subunit of the phosphatase and MLC, which leads to myosin contraction (4, 39, 44) and the associated formation of stress fibers and focal adhesions (2, 37, 47). In addition to its effect on actin microfilaments, RhoA induces changes in the IF network (60) and has recently been shown to stabilize MTs (16). Here, we show that overexpression of ROKα caused the collapse of the vimentin IF network into tight bundles with no apparent disassembly of the microtubular network, in addition to the formation of stress fibers. Since the RhoA-binding-deficient, kinase-dead ROKα inhibits the collapse of IFs induced by overexpression of RhoA, ROKα is probably working downstream of RhoA in affecting the state of IFs. PKN has recently been shown to associate with and to phosphorylate the neurofilament proteins (56). Rho-associated kinase phosphorylates GFAP, an IF protein expressed in astroglia (41). Thus, ROKα is part of a rapidly enlarging family of RhoA-binding kinases that can potentially affect the structural integrity of the IFs.

Disassembly of the vimentin IF network induced by PKA can progress from the state of collapsed bundles to punctate clusters throughout the cytoplasm (45). This disassembly, which probably requires conformational changes in vimentin, is accompanied by increased vimentin phosphorylation (13, 45) and is apparently regulated by site-specific phosphorylation at the head domain of vimentin (13). The phosphorylation sites on the head domain of GFAP of Rho-associated kinase/ROKα and PKA are nearly identical (41, 68). While the manuscript was being reviewed, Goto et al. (27) reported that Rho-kinase (ROKα) phosphorylates vimentin at Ser38 and Ser71, although Ser71 does not appear to be phosphorylated in interphase cells. Since Ser38 is also one of the major PKA phosphorylation sites (25, 68), it is then not surprising that both ROKα and PKA can inhibit polymerization of vimentin in vitro (Fig. 2D). Although phosphorylated vimentin often remains soluble in vitro (12, 33), there is no increase in soluble vimentin in fibroblasts upon PKA-induced collapse of IFs (45), perhaps because of the presence of IF-associated proteins, which prevents complete disassembly of the filamentous network in vivo. Recently, the use of green fluorescent protein-tagged vimentin showed that collapse of IF bundles did not necessarily involve reassembly near the nucleus but rather the network being pushed back into the perinuclear region (31).

Our finding that ROKα colocalizes with intact vimentin IFs in Swiss 3T3 fibroblasts, probably in a catalytically inactive form (see above), is in keeping with reports that many kinases appear to cluster around their sites of action and to associate with various cellular structures including cytoskeletal elements. Mixed-lineage kinase 2, for example, has been found to colocalize with MTs (57), and a number of kinases such as cyclic GMP-dependent protein kinase and PKC have a high affinity for vimentin (51, 66, 73). When IFs were induced to collapse by MT-disrupting agents or in the presence of RhoA-activating factors, ROKα translocated to the cell periphery. Active RhoA is necessary for ROKα translocation since, in SPP- and vinblastine-treated HeLa cells, overexpression of the dominant-negative mutant of RhoA inhibits the translocation. An intact filamentous structure, presumably comprised largely of nonphosphorylated vimentin, is apparently required for the continued association of ROKα with vimentin IFs. Inactive ROKα (the kinase-dead mutant) has low affinity for phosphorylated vimentin, suggesting that translocation of ROKα may be facilitated by its dissociation from vimentin filaments when vimentin is phosphorylated.

In SPP-treated cells, translocated ROKα overlaps partially with vinculin at the cell periphery. Indeed, RhoA is necessary to promote vinculin association with the plasma membrane, and this could be mediated by ROKα (11, 47). Several lines of evidence suggest that membrane binding of ROKα is required for its activation. For example, translocation of ROKα to target regions is essential for it to induce neurite retraction in PC12 cells (38). ROCK (an isoenzyme of ROKα) translocates to membrane-cytoskeletal complexes upon cell stimulation (24). Once at the membrane, it is not known whether other domains of ROKα, such as the PH domain, assist in its anchorage, as in the case of SOS, whose PH domain is required for membrane association (10). RhoA appears to localize ezrin/radixin/moesin (ERM) to the apical membrane (65), and its stimulation of ERM phosphorylation has been shown to be mediated by ROKα (55). The latter authors suggest that ROKα has a direct role in opening up ERM proteins to facilitate interaction with actin, which could help in the anchoring of stress fibers.

We propose that translocation of ROKα to its sites of action may involve its release from the IFs only when they are induced to collapse by phosphorylation, as part of a coordinated cytoskeletal response to extracellular stimuli (Fig. 8). In serum-starved cells, ROKα in its inactivated form is preferentially bound to IFs. Some ROKα may be present as unbound form in the cytosol or at the membrane. These cells would be expected

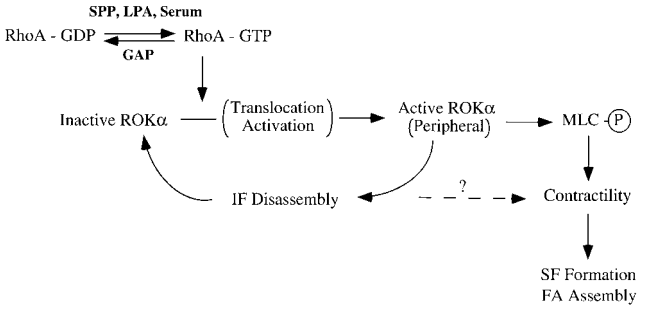

FIG. 8. A role for vimentin IFs as a reservoir of ROKα. Activated ROKα performs many roles; two of those are shown here for simplicity. Generation of RhoA-GTP by growth factors results in initial activation of a free pool of ROKα. Activated ROKα then phosphorylates vimentin on IFs, leading to the release of inactive ROKα, because of its reduced affinity for vimentin which is phosphorylated. The released ROKα is translocated to the periphery, where it is activated upon binding to RhoA-GTP. This activated ROKα acts on IFs to accelerate their phosphorylation-disassembly, thus releasing more ROKα to be activated in a positive feedback loop. Activated ROKα also induces an overall increase in phosphorylated MLC, from either the inactivation of myosin phosphatase or the phosphorylation of MLC. These events lead to an increase in myosin-based contractility and the subsequent formation of stress fibers (SF) and assembly of focal adhesions (FA). It is possible that contractility may also be enhanced by the disassembly of IFs. GAP, GTPase-activating protein.

to contain much of its RhoA in the GDP form. Exposure to serum, SPP, or LPA (the latter two being also present in serum) results in conversion of RhoA to the active GTP-bound form, which then activates ROKα. Because RhoA can be found in the membrane and cytosol irrespective of its state of activation (6, 43, 69, 70), it is not clear which subcellular pool of ROKα is initially activated by RhoA. In any case, this activated ROKα then phosphorylates vimentin, which has a reduced affinity for ROKα, thus releasing it. This released ROKα is then translocated and activated, most probably on the peripheral membrane, and acts on vimentin, resulting in yet more phosphorylation and further release of previously bound ROKα. The collapse of IFs alone may be sufficient to release ROKα for translocation, as heat shock induced redistribution of ROKα to the periphery without an accompanying increase in stress fibers. However, kinase activity of ROKα is necessary to bring about the collapse since the kinase-dead mutant inhibits vinblastine-induced collapse of IFs. ROKα appears to be in a positive feedback loop such that increased amounts of ROKα could be translocated to the cell edge, with the IFs acting as a depository for ROKα. Receipt of additional signals that decrease the level of RhoA-GTP, for instance, increased RhoGAP activity, will terminate the feedback loop. The increase in contractility, which mostly results from the phosphorylation of myosin binding subunit of phosphatase and of MLC itself by ROKα, may be facilitated by the collapse of IFs. It is possible that the formation of stress fibers, focal adhesions, and contractility observed on MT disruption (19, 75) reflects not a direct activation of Rho but rather an associated release of ROK from IFs and its subsequent translocation (Fig. 5B) and activation.

There is increasing evidence to suggest that regulating the dynamics of IFs is important in various cellular processes (20, 23). Stability of vimentin IFs is necessary for maintaining nuclear morphology (63) and that of other cytoskeletal constituents, including actin microfilaments. Thus, unregulated destabilization of vimentin IFs by microinjection of a mimetic peptide, whose sequence corresponds to that of the N-terminal helical initiation 1A of vimentin, into fibroblasts causes condensation of actin into large aggregates and cell rounding (26). Cross-talk between IF and other cytoskeletal components is evident, as in the treatment of adrenal cells with calcium-calmodulin, which results in cell rounding and the phosphorylation of both vimentin and MLC (1). In vimentin knockout mice, which do not have an obvious phenotype but nevertheless possess fragile fibroblasts (15, 26), it is possible that there may be compensatory expression of other cytoskeletal elements. Furthermore, vimentin-deficient fibroblasts have recently been shown to have impaired mechanical stability and contractility (18).

It is clear that ROKα can influence diverse cytoskeletal events, including contractility of myosin, the reorganization of actin filaments, the structural status of IFs, and the regulation of ERM. While this paper was being reviewed, it was reported that ROCK influences the assembly of IFs, MTs, and actomyosin-based contractility in neuronal cells (30). It is not unlikely that a common signal can affect both the state of IFs and actomyosin contraction, which has been proposed to underlie formation of stress fibers and focal adhesions. Extensive IF disassembly is unlikely to occur in normal nondividing cells; however, localized IF phosphorylation could modulate the structure of IFs in specific areas of interphase cells undergoing cytoskeletal changes. It is possible that ROKα has a role in coordinating different components of the cytoskeleton, contributing to a change in cell shape which requires the concerted movement of major cytoskeletal elements.

ACKNOWLEDGMENT

We thank the Glaxo-Singapore Research Fund for support.

REFERENCES

1. **Almahbobi, G., M. Korn, and P. F. Hall.** 1994. Calcium/calmodulin induces phosphorylation of vimentin and myosin light chain and cell rounding in cultured adrenal cells. Eur. J. Cell Biol. **63:**307–315.
2. **Amano, M., K. Chihara, K. Kimura, Y. Fukata, N. Nakamura, Y. Matsuura, and K. Kaibuchi.** 1997. Formation of actin stress fibers and focal adhesions enhanced by Rho-kinase. Science **275:**1308–1311.
3. **Amano, M., H. Mukai, Y. Ono, K. Chihara, T. Matsui, Y. Hamajima, K. Okawa, A. Iwamatsu, and K. Kaibuchi.** 1996. Identification of a putative target for Rho as the serine-threonine kinase protein kinase N. Science **271:**648–650.
4. **Amano, M., M. Ito, K. Kimura, Y. Fukata, K. Chihara, T. Nakano, Y. Matsuura, and K. Kaibuchi.** 1996. Phosphorylation and activation of myosin by Rho-associated kinase (Rho-kinase). J. Biol. Chem. **271:**20246–20249.
5. **Bershadsky, A., A. Chausovsky, E. Becker, A. Lyubimova, and B. Geiger.** 1996. Involvement of microtubules in the control of adhesion-dependent signal transduction. Curr. Biol. **6:**1279–1289.
6. **Boukharov, A. A., and C. M. Cohen.** 1998. Guanine nucleotide-dependent translocation of RhoA from cytosol to high affinity membrane binding sites in human erythrocytes. Biochem. J. **330:**1391–1398.
7. **Burridge, K., M. Chrzanowska-Wodnicka, and C. Zhong.** 1997. Focal adhesion assembly. Trends Cell Biol. **7:**342–347.
8. **Capetanaki, Y., I. Kuisk, K. Rothblum, and S. Starnes.** 1990. Mouse vimentin: structural relationship to fos, jun, CREB, and tpr. Oncogene **5:**645–655.
9. **Chen, C., and H. Okayama.** 1987. High-efficiency transformation of mammalian cells by plasmid DNA. Mol. Cell. Biol. **7:**2745–2752.
10. **Chen, R.-H., S. Corbalan-Garcia, and D. Bar-Sagi.** 1997. The role of the PH domain in the signal-dependent membrane targeting of Sos. EMBO J. **16:** 1351–1359.
11. **Chihara, K., M. Amano, N. Nakamura, T. Yano, M. Shibata, T. Tokui, H. Ichikawa, R. Ikebe, M. Ikebe, and K. Kaibuchi.** 1997. Cytoskeletal rearrangements and transcriptional activation of c-fos serum response element by Rho-kinase. J. Biol. Chem. **272:**25121–25127.
12. **Chou, Y.-H., E. Rosevear, and R. D. Goldman.** 1989. Phosphorylation and disassembly of intermediate filaments in mitotic cells. Proc. Natl. Acad. Sci. USA **86:**1885–1889.
13. **Chou, Y.-H., P. Opal, R. A. Quinlan, and R. D. Goldman.** 1996. The relative roles of specific N- and C-terminal phosphorylation sites in the disassembly of intermediate filament in mitotic BHK-21 cells. J. Cell Sci. **109:**817–826.
14. **Chrzanowska-Wodnicka, M., and K. Burridge.** 1996. Rho-stimulated contractility drives the formation of stress fibers and focal adhesions. J. Cell Biol. **133:**1403–1415.
15. **Colucci-Guyon, E., M.-M. Portier, I. Dunia, D. Paulin, S. Pournin, and C. Babinet.** 1994. Mice lacking vimentin develop and reproduce without an

obvious phenotype. Cell **79:**679–694.
16. **Cook, T. A., T. Nagasaki, and G. G. Gundersen.** 1998. Rho guanosine triphosphatase mediates the selective stabilization of microtubules induced by lysophosphatidic acid. J. Cell Biol. **141:**175–185.
17. **Danowski, B. A.** 1989. Fibroblast contractility and actin organization are stimulated by microtubule inhibitors. J. Cell Sci. **83:**255–266.
18. **Eckes, B., D. Dogic, E. Colucci-Guyon, N. Wang, A. Maniotis, D. Ingber, A. Merckling, F. Langa, M. Aumailley, A. Delouvee, V. Koteliansky, C. Babinet, and T. Krieg.** 1998. Impaired mechanical stability, migration and contractile capacity in vimentin-deficient fibroblasts. J. Cell Sci. **111:**1897–1907.
19. **Enomoto, T.** 1996. Microtubule disruption induces the formation of actin stress fibers and focal adhesions in cultured cells: possible involvement of the Rho signal cascade. Cell Struct. Funct. **21:**317–326.
20. **Foisner, R.** 1997. Dynamic organisation of intermediate filaments and associated proteins during the cell cycle. Bioessays **19:**297–305.
21. **Foisner, R., F. E. Leichtfried, H. Herrmann, J. V. Small, D. Lawson, and G. Wiche.** 1988. Cytoskeleton-associated plectin: in situ localization, *in vitro* reconstitution, and binding to immobilized intermediate filament proteins. J. Cell. Biol. **106:**723–733.
22. **Franke, W. W., E. Schmid, M. Osborn, and K. Weber.** 1978. Different intermediate-sized filaments distinguished by immunofluorescence microscopy. Proc. Natl. Acad. Sci. USA **75:**5034–5038.
23. **Fuchs, E., and K. Weber.** 1994. Intermediate filaments: structure, dynamics, function and disease. Annu. Rev. Biochem. **63:**345–382.
24. **Fujita, A., Y. Saito, T. Ishizaki, M. Maekawa, K. Fujisawa, F. Ushikubi, and S. Narumiya.** 1997. Integrin-dependent translocation of p160ROCK to cytoskeletal complex in thrombin-stimulated human platelets. Biochem. J. **328:**769–775.
25. **Geisler, N., M. Hatzfeld, and K. Weber.** 1989. Phosphorylation *in vitro* of vimentin by protein kinases A and C is restricted to the head domain. Eur. J. Biochem. **183:**441–447.
26. **Goldman, R. D., S. Khuon, Y. H. Chou, P. Opal, and P. M. Steinert.** 1996. The function of intermediate filaments in cell shape and cytoskeletal integrity. J. Cell Biol. **134:**971–983.
27. **Goto, H., H. Kosako, K. Tanabe, M. Yanagida, M. Sakurai, M. Amano, K. Kaibuchi, and M. Inagaki.** 1998. Phosphorylation of vimentin by Rho-associated kinase at a unique amino-terminal site that is specifically phosphorylated during cytokinesis. J. Biol. Chem. **273:**11728–11736.
28. **Gyoeva, F. K., and V. I. Gelfand.** 1991. Coalignment of vimentin intermediate filaments with microtubules depends on kinesin. Nature (London) **353:** 445–448.
29. **Hall, A.** 1998. Rho GTPases and the actin cytoskeleton. Science **279:**509–514.
30. **Hirose, M., T. Ishizaki, N. Watanabe, M. Uehata, O. Kranenburg, W. H. Moolenaar, F. Matsumura, M. Maekawa, H. Bito, and S. Narumiya.** 1998. Molecular dissection of the Rho-associated protein kinase (p160ROCK)-regulated neurite remodeling in neuroblastoma N1E-115 cells. J. Cell Biol. **141:**1625–1636.
31. **Ho, C.-L., J. L. Martys, A. Mikhailov, G. G. Gundersen, and R. K. H. Liem.** 1998. Novel features of intermediate filament dynamics revealed by green fluorescent protein chimeras. J. Cell Sci. **111:**1767–1778.
32. **Hollenbeck, P. J., A. D. Bershadsky, O. Y. Pletjushkina, I. S. Tint, and J. M. Vasiliev.** 1989. Intermediate filament collapse is an ATP-dependent and actin-dependent process. J. Cell Sci. **92:**621–631.
33. **Inagaki, M., Y. Gonda, M. Matsuyama, K. Nishizawa, Y. Nishi, and C. Sato.** 1988. Intermediate filament reconstitution *in vitro*. J. Biol. Chem. **263:**5970–5978.
34. **Inagaki, M., Y. Matsuoka, K. Tsujimura, S. Ando, T. Tokui, T. Takahashi, and N. Inagaki.** 1996. Dynamic property of intermediate filaments: regulation by phosphorylation. Bioessays **18:**481–487.
35. **Inagaki, M., Y. Nishi, K. Nishizawa, M. Matsuyama, and C. Sato.** 1987. Site-specific phosphorylation induces disassembly of vimentin filaments *in vitro*. Nature (London) **328:**649–652.
36. **Ishizaki, T., M. Maekawa, K. Fujisawa, K. Okawa, A. Iwamatsu, A. Fujita, N. Watanabe, Y. Saito, A. Kakizuka, N. Morii, and S. Narumiya.** 1996. The small GTP-binding protein Rho binds to and activates a 160 kDa Ser/Thr protein kinase homologous to myotonic dystrophy kinase. EMBO J. **15:** 1885–1893.
37. **Ishizaki, T., M. Naito, K. Fujisawa, M. Maekawa, N. Watanabe, Y. Saito, and S. Narumiya.** 1997. p160ROCK, a Rho-associated coiled-coil forming protein kinase, works downstream of Rho and induces focal adhesions. FEBS Lett. **404:**118–124.
38. **Katoh, H., J. Aoki, A. Ichikawa, and M. Negishi.** 1998. p160 RhoA-binding kinase ROKα induces neurite retraction. J. Biol. Chem. **273:**2489–2492.
39. **Kimura, K., M. Ito, M. Amano, K. Chihara, Y. Fukata, M. Nakafuku, B. Yamamori, J. Feng, T. Nakano, K. Okawa, A. Iwamatsu, and K. Kaibuchi.** 1996. Regulation of myosin phosphatase by Rho and Rho-associated kinase (Rho-kinase). Science **273:**245–248.
40. **Kolodney, M. S., and E. L. Elson.** 1995. Contraction due to microtubule disruption is associated with increased phosphorylation of myosin regulatory light chain. Proc. Natl. Acad. Sci. USA **92:**10252–10256.
41. **Kosako, H., M. Amano, M. Yanagida, K. Tanabe, Y. Nishi, K. Kaibuchi, and M. Inagaki.** 1997. Phosphorylation of glial fibrillary acidic protein at the same sites by cleavage furrow kinase and Rho-associated kinase. J. Biol. Chem. **272:**10333–10336.
42. **Kozma, R., S. Ahmed, A. Best, and L. Lim.** 1995. The Ras-related protein Cdc42Hs and bradykinin promote formation of peripheral actin microspikes and filopodia in Swiss 3T3 fibroblasts. Mol. Cell. Biol. **15:**1942–1952.
43. **Kranenburg, O., M. Poland, M. Gebbink, L. Oomen, and W. H. Moolenaar.** 1997. Dissociation of LPA-induced cytoskeletal contraction from stress fiber formation by differential localization of RhoA. J. Cell Sci. **110:**2417–2427.
44. **Kureishi, Y., S. Kobayashi, M. Amano, K. Kimura, H. Kanaide, T. Nakano, K. Kaibuchi, and M. Ito.** 1997. Rho-associated kinase directly induces smooth muscle contraction through myosin light chain phosphorylation. J. Biol. Chem. **272:**12257–12260.
45. **Lamb, N. J. C., A. Fernandez, J. R. Feramisco, and W. J. Welch.** 1989. Modulation of vimentin containing intermediate filament distribution and phosphorylation in living fibroblasts by the cAMP-dependent protein kinase. J. Cell Biol. **108:**2409–2422.
46. **Leung, T., E. Manser, L. Tan, and L. Lim.** 1995. A novel serine/threonine kinase binding the ras-related RhoA GTPases which translocates the kinase to peripheral membranes. J. Biol. Chem. **270:**29051–29054.
47. **Leung, T., X.-Q. Chen, E. Manser, and L. Lim.** 1996. The p160 RhoA-binding kinase ROKα is a member of a kinase family and is involved in the reorganization of the cytoskeleton. Mol. Cell. Biol. **16:**5313–5327.
48. **Leung, T., X.-Q. Chen, I. Tan, E. Manser, and L. Lim.** 1998. Myotonic dystrophy kinase-related cdc42-binding kinase acts as a cdc42 effector in promoting cytoskeletal reorganization. Mol. Cell. Biol. **18:**130–140.
49. **Lim, L., E. Manser, T. Leung, and C. Hall.** 1996. Regulation of phosphorylation pathways by p21 GTPases. Eur. J. Biochem. **242:**171–185.
50. **Machesky, L. M., and A. Hall.** 1997. Role of actin polymerization and adhesion to extracellular matrix in rac- and rho-induced cytoskeletal reorganization. J. Cell Biol. **138:**913–926.
51. **MacMillan-Crow, L. A., and T. M. Lincoln.** 1994. High-affinity binding and localization of the cyclic GMP-dependent protein kinase with the intermediate filament protein vimentin. Biochemistry **33:**8035–8043.
52. **Manser, E., H.-Y. Huang, T.-H. Loo, X.-Q. Chen, J.-M. Dong, T. Leung, and L. Lim.** 1997. Expression of constitutively active α-PAK reveals effects of the kinase on actin and focal complexes. Mol. Cell. Biol. **17:**1129–1143.
53. **Manser, E., T. Leung, H. Salihuddin, Z.-S. Zhao, and L. Lim.** 1994. A brain serine/threonine protein kinase activated by Cdc42 and Rac1. Nature (London) **367:**40–46.
54. **Matsui, T., M. Amano, T. Yamamoto, K. Chihara, M. Nakafuku, M. Ito, T. Nakano, K. Okawa, A. Iwamatsu, and K. Kaibuchi.** 1996. Rho-associated kinase, a novel serine/threonine kinase, as a putative target for the small GTP binding protein Rho. EMBO J. **15:**2208–2216.
55. **Matsui, T., M. Maeda, Y. Doi, S. Yonemura, M. Amano, K. Kaibuchi, S. Tsukita, and S. Tsukita.** 1998. Rho-kinase phosphorylates COOH-terminal threonines of ezrin/radixin/moesin (ERM) proteins and regulates their head-to-tail association. J. Cell Biol. **140:**647–657.
56. **Mukai, H., M. Toshimori, H. Shibata, M. Kitagawa, M. Shimakawa, M. Miyahara, H. Sunakawa, and Y. Ono.** 1996. PKN associates and phosphorylates the head-rod domain of neurofilament protein. J. Biol. Chem. **271:** 9816–9822.
57. **Nagata, K., A. Puls, C. Futter, P. Aspenstrom, E. Schaefer, T. Nataka, N. Hirokawa, and A. Hall.** 1998. The MAP kinase kinase kinase MLK2 co-localizes with activated JNK along microtubules and associates with kinesin superfamily motor KIF3. EMBO J. **17:**149–158.
58. **Nobes, C. D., and A. Hall.** 1995. Rho, Rac, and Cdc42 GTPases regulate the assembly of multimolecular focal complexes associated with actin stress fibers, lamellipodia and filopodia. Cell **81:**53–62.
59. **Osborn, M., and K. Weber.** 1982. Immunofluorescence and immunocytochemical procedures with affinity purified antibodies: tubulin-containing structures. Methods Cell Biol. **24:**97–132.
60. **Paterson, H. F., A. F. Self, M. D. Garrett, I. Just, K. Aktories, and A. Hall.** 1990. Microinjection of recombinant $p21^{rho}$ induces rapid changes in cell morphology. J. Cell Biol. **111:**1001–1007.
61. **Ridley, A. J., and A. Hall.** 1992. The small GTP binding protein rho regulates the assembly of focal adhesions and actin stress fibers in response to growth factors. Cell **70:**389–399.
62. **Ridley, A. J., H. F. Paterson, C. L. Johnston, D. Diekmann, and A. Hall.** 1992. The small GTP-binding protein rac regulates growth factor-induced membrane ruffling. Cell **70:**401–410.
63. **Sarria, A. J., J. G. Lieber, S. K. Nordeen, and R. M. Evans.** 1994. The presence or absence of a vimentin-type intermediate filament network affects the shape of the nucleus in human SW-13 cells. J. Cell Sci. **107:**1593–1607.
64. **Sells, M. A., U. F. Knaus, S. Bagrodia, D. M. Ambrose, G. M. Bokoch, and J. Chernoff.** 1997. Human p21-activated kinase (Pak1) regulates actin organization in mammalian cells. Curr. Biol. **7:**202–210.
65. **Shaw, R. J., M. Henry, F. Solomon, and T. Jacks.** 1998. RhoA-dependent phosphorylation and relocalization of ERM proteins into apical membrane/actin protrusions in fibroblasts. Mol. Biol. Cell **9:**403–419.
66. **Spudich, A., T. Meyer, and L. Stryer.** 1992. Association of the beta isoform

of protein kinase C with vimentin filaments. Cell Motil. Cytoskelet. **22:**250–256.

67. **Suga, S., M. Tsurudome, S. Ohgimoto, N. Tabata, N. Watanabe, M. Nishio, M. Kawano, H. Komada, M. Sakurai, and Y. Ito.** 1996. Intracellular localization of antigens recognized by anti-vimentin monoclonal antibodies (mAbs): cross-reactivities of anti-vimentin mAbs with other cellular components. Eur. J. Cell Biol. **70:**84–91.
68. **Takai, Y., N. Inagaki, O. Tsutsumi, and M. Inagaki.** 1996. Visualization and regulation of intermediate filament kinase activities. Semin. Cell Dev. Biol. **7:**741–749.
69. **Takaishi, K., T. Sasaki, T. Kameyama, S. Tsukita, S. Tsukita, and Y. Takai.** 1995. Translocation of activated Rho from the cytoplasm to membrane ruffling area, cell-cell adhesion sites and cleavage furrows. Oncogene **11:**39–48.
70. **Takaishi, K., T. Sasaki, H. Kotani, H. Nishioka, and Y. Takai.** 1997. Regulation of cell-cell adhesion by Rac and Rho small G proteins in MDCK cells. J. Cell Biol. **139:**1047–1059.
71. **Van Aelst, L., and C. D'Souza-Schorey.** 1997. Rho GTPases and signaling networks. Genes Dev. **11:**2295–2322.
72. **Welch, W. J., and J. P. Suhan.** 1985. Morphological study of the mammalian stress response: characterization of changes in cytoplasmic organelles, cytoskeleton, and nucleoli, and appearance of intranuclear actin filaments in rat fibroblasts after heat-shock treatment. J. Cell Biol. **101:**1198–1211.
73. **Wyatt, T. A., T. M. Lincoln, and K. B. Pryzwansky.** 1991. Vimentin is transiently colocalized with and phosphorylated by cyclic GMP-dependent protein kinase in formyl-peptide-stimulated neutrophils. J. Biol. Chem. **266:**21274–21280.
74. **Zackroff, R. V., and R. D. Goldman.** 1979. *In vitro* assembly of intermediate filaments from baby hamster kidney (BHK-21) cells. Proc. Natl. Acad. Sci. USA **76:**6226–6230.
75. **Zhang, Q., M. K. Magnusson, and D. F. Mosher.** 1997. Lysophosphatidic acid and microtubule-destabilizing agents stimulate fibronectin matrix assembly through Rho-dependent actin stress fiber formation and cell contraction. Mol. Biol. Cell **8:**1415–1425.